JOURNAL OF VIROLOGY, Sept. 1996, p. 5867–5874 Vol. 70, No. 9
0022-538X/96/$04.00+0

Analysis of Early Region 3 Mutants of Mouse Adenovirus Type 1

CLAYTON W. BEARD† AND KATHERINE R. SPINDLER*

Department of Genetics, University of Georgia, Athens, Georgia 30602

Received 24 April 1996/Accepted 3 June 1996

Early region 3 (E3) of mouse adenovirus type 1 has the potential to produce three proteins which have identical amino termini but unique carboxy-terminal sequences. Three recombinant deletion viruses were constructed so that each could produce only one of the three E3 proteins. A fourth mutant that should produce no E3 proteins was also constructed. These recombinants were able to grow in mouse 3T6 cells and produced wild-type levels of viral mRNAs and proteins except for those specifically deleted by the mutations. Early mRNA production from the mutant viruses was analyzed by reverse transcriptase PCR and confirmed that each deletion mutant would be able to produce only one of the three E3 proteins. Late mRNA production was analyzed by Northern (RNA) blotting and found to be similar in wild-type and mutant viruses. Capsid morphology was unaltered in the mutant viruses as seen by electron microscopy. Immunoprecipitation of E3 proteins from infections of mouse 3T6 cells using an antiserum specific for all three E3 proteins was used to examine the effect of the introduced mutations on protein expression. Two mutants produced only one class of E3 protein as predicted from their specific mutations and mRNA expression profiles. One mutant virus failed to produce any detectable E3 proteins. The predicted E3-null mutant was found to be leaky and could produce low levels of E3 proteins. Outbred Swiss mice were infected with the E3 mutant viruses to determine if the E3 proteins have an effect on the pathogenicity of the virus in mice. All of the mutants showed decreased pathogenicity as determined by increased 50% lethal doses, indicating that the proteins of the E3 region are important determinants of the pathogenesis of mouse adenovirus in its natural host.

Early region 3 (E3) has been found in all of the adenoviruses identified to date. Although this region has been maintained through the evolution of adenoviruses, it is the most highly variant region among different subgenera of adenoviruses. This variation may correlate with the differences in the pathogenicity of these serotypes (2). Human adenovirus 2 (Ad2) E3 has been studied extensively and has been shown to be nonessential for virus growth in cell culture (33). This region has been implicated in mediating the interactions between the infected cell and the host immune response (53). The E3 proteins of adenovirus 2 and 5 (Ad2/5), which can cause acute pharyngitis in humans, have been well characterized and found to have functions that could be important in virus-host interactions.

The Ad2/5 gp19K is the predominant protein produced from the E3 region during an infection (39). This protein is localized to the endoplasmic reticulum, where it binds to and retains the class 1 antigens of the major histocompatibility complex (MHC) (1, 10, 21). Retention of class 1 MHC in the endoplasmic reticulum may enable adenoviruses to evade the T-cell-mediated immune response (11, 12) and contribute to the ability of these viruses to cause persistent infections (38). Other E3 proteins that interact with immune mechanisms are the Ad2/5 E3 14.7K and 10.4K/14.5K proteins. These proteins protect infected cells from cytolysis by tumor necrosis factor (TNF) (24, 25, 49, 50). The E3 10.4K protein has been shown to down-regulate the expression of epidermal growth factor receptors on the surface of infected cells (14). The E3 11.6K protein has recently been designated as the human adenovirus death protein because of its ability to promote the lysis of human adenovirus-infected cells (48).

The role that the E3 proteins play in infections of the natural host has been difficult to determine because of the species specificity of adenoviruses. Several approaches have been used to facilitate studies of these proteins. One is the use of the cotton rat as a model system for human adenovirus infection. Cotton rats infected intranasally with wild-type (wt) Ad5 develop a pulmonary infection. Infection of cotton rats by a mutant Ad5 that lacks the E3 gp19K protein results in increased lung inflammation (22). It has not been shown that gp19K can interact with the cotton rat class 1 MHC protein; thus, it is not possible to attribute the altered pathogenicity to the lack of gp19K interaction with class 1 MHC. In a second model, human adenovirus is unable to replicate in mouse cells, but at high doses it can cause murine pneumonia (23). This model has been used to evaluate the pathology caused by mutant viruses that lack either gp19K or the E3 functions involved in TNF protection. Experiments in human adenovirus-infected mice demonstrated that the 14.7K and 10.4K/14.5K E3 proteins reduce the recruitment of inflammatory cells into the alveoli of the lungs, while gp19K is incapable of altering the immune response (46).

Another approach to studying the role of the E3 proteins in vivo has been to insert their genes into vaccinia virus and study the pathogenesis of this virus in mice. These experiments showed that the gp19K protein has no effect on the pathogenesis of vaccinia virus (16, 27). Similar experiments have been conducted to investigate the ability of the E3 14.7K protein to alter vaccinia virus pathogenicity (49). Viruses used in this study contained either the TNF gene alone or both the TNF gene and the E3 14.7K gene. Viruses that express only the TNF protein are attenuated in the mouse, while those expressing both the TNF and the 14.7K proteins are not. The ability of 14.7K to counteract the antiviral activity of TNF in vivo sup-

* Corresponding author. Phone: (706) 542-8395. Fax: (706) 542-3910. Electronic mail address: spindler@uga.cc.uga.edu.

† Present address: Plum Island Animal Disease Center, Agricultural Research Service, U.S. Department of Agriculture, Greenport, NY 11944.

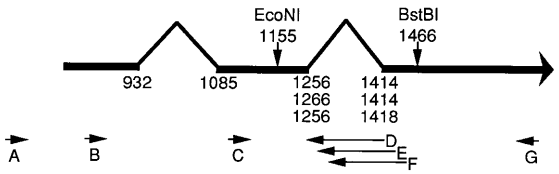

FIG. 1. Restriction sites and primers of the E3 region. Thick line, mRNA; angles, introns. PCR primers: A, MAVRneg27; B, MAVR851; C, MAVR1098; D, MAVRC1; E, MAVRC2; F, MAVRC3; G, MAVR1508. Nucleotide positions of splice sites are indicated.

ports the hypothesis that this protein has a role in adenovirus evasion of the host immune system.

We used mouse adenovirus (MAV-1) to study the function of E3 proteins in viral pathogenesis because MAV-1 can be studied in the natural host and because MAV-1 has some similarity to the human adenoviruses (3, 4, 6, 13, 15, 35, 37, 40, 44, 52). The E3 region of MAV-1 encodes three transcripts that are predicted to produce three different E3 proteins (6). One of the MAV-1 E3 proteins, gp11K, is a peripheral membrane glycoprotein that is localized to the endoplasmic reticulum (7). The other two predicted E3 proteins have not been identified in wt MAV-1-infected cultured cells.

We have developed a method that allows directed mutagenesis of the MAV-1 genome and have produced viral recombinants with various defects in E3 expression. We describe the construction of these viral mutants and their characterization in both cell culture and mice. Evidence presented here indicates that the E3 proteins of MAV-1 play an important role in the pathogenesis of this virus in its natural host.

MATERIALS AND METHODS

Construction of E3 mutant plasmids. cDNA clones of mRNAs that encode the MAV-1 E3 protein gp11K (clone pZ70) or predicted class 2 (pZ50) or class 3 (pZ333.6) proteins were digested with *Eco*NI at nucleotide (nt) 1155 and *Bst*BI at nt 1466 (6) (Fig. 1). The resulting DNA fragments that contained the specific splice junction of the second intron from each E3 cDNA were isolated and ligated into the MAV-1 genomic clone pBHC-2 (nt 779 to 3657 [GenBank accession no. M30594] in pBS+) (Stratagene) that had been digested with *Eco*NI at nt 1155 and *Bst*BI at nt 1466. These plasmids were designated pCEX-1, pCEX-2, and pCEX-3 for gp11K, class 2, and class 3 respectively. Oligonucleotide site-directed mutagenesis (Amersham) was used to construct the E3-null mutant plasmid p4×MUT as follows. An oligonucleotide (MAVR876, CTCTT TCTGCAAGCTTGTCCGAATTGAGCGGGGC [876 designates the sequence position of the 5′ end]) (obtained from Operon Technologies, Inc.) was designed to change the ATG initiator sequences at nt 890 and 899 to TTG. This introduced a conservative amino acid change from methionine to leucine in the coding sequence of the late protein pVIII, which overlaps the 5′ portion of the E3 region. Two additional oligonucleotides, MAVR1449 (GGGGCAAGACTG CAGTTCGAACTGG) and MAVR1596 (GTTCTGGCTGGTACCGCTGAAG TAATC), were designed to construct a mutant that would eliminate the possibility of downstream initiation from ATGs at nt 1458 and 1605, respectively. MAVR876 created a new *Hin*dIII site, MAVR1449 created a new *Pst*I site, and MAVR1596 created a new *Kpn*I site. These new restriction sites were used to screen for the incorporation of the mutations into both plasmids and viral recombinants. All three oligonucleotides were used to mutate the plasmid pMUT-1 (43), which contains a MAV-1 genomic fragment from nt 1 to 3657 of the E3 region (40) (GenBank accession no. M30594). Oligonucleotide site-directed mutagenesis was also used to create the plasmid pMUT-3 as follows. The plasmid pMXD containing the MAV-1 genomic sequence from 0 to 12 map units (nt 1 to 3700 in E1) (4) was mutagenized with the oligonucleotide E1BR1 (CTACAGAATTGCCTACCACAG). This oligonucleotide contained a single base change at nt 2373 that abolished the *Eco*RI recognition sequence while maintaining the proper coding sequence for the E1B 55K protein encoded by this region.

Production of MAV-1 recombinant viruses. pMUT-3 was treated with T7 gene 6 exonuclease (34) to produce single-stranded DNA. This was then annealed to a MAV-1 genomic viral DNA complex (19) that had been partially digested with exonuclease III. The DNA was then transfected into mouse L929 cells by the calcium phosphate precipitation method (26). Virus plaques were isolated and amplified to a high enough level to allow enough viral DNA to be isolated by the Hirt method (32). This DNA was then analyzed by digestion with *Eco*RI and *Hin*dIII. Potential mutants were further verified by differential Southern blotting with the E1BR1 oligonucleotide (45). The *Eco*RI mutant virus, designated *pm*E101, was plaque purified three times and grown into a virus stock. To construct E3 mutants, *pm*E101 viral DNA-protein complex was isolated, digested with *Eco*RI, and partially filled in by using Klenow polymerase as follows. Ten micrograms of the DNA-protein complex was digested with 80 U of *Eco*RI in a volume of 500 μl. dATP was added to a final concentration of 0.3 mM, 12 U of DNA polymerase Klenow fragment was added, and the reaction mixture was incubated at 30°C for 30 min. This partial fill-in prevented religation of the *Eco*RI cohesive ends and forced recombination between the viral DNA and plasmid DNA to yield viable virus. Mouse 3T6 cells were cotransfected with plasmid DNA (5 μg) from pCEX-1, pCEX-2, pCEX-3, or p4×MUT and 2 μg of a treated *pm*E101 complex. Virus plaques were isolated, identified by restriction digests, and verified by PCR and sequencing (see below). The recombinant viruses are listed in Fig. 2.

mRNA isolation and Northern blot analysis. Mouse 3T6 cells were grown as described elsewhere (4) and infected with virus at a multiplicity of 1 PFU per cell or were mock infected with phosphate-buffered saline. Total RNA was isolated, and 20 μg was Northern (RNA) blotted as previously described (3). Probes for Northern blotting were random-primer-labeled DNAs of plasmids pATE, pFiber, and pZU14. Plasmid pATE contains the MAV-1 DNA fragment from nt 475 to 745 of sequence in the pVIII/E3 region (6, 40) inserted into pBluescript II SK$^-$ (Stratagene). This sequence is the pVIII (L4) region. Plasmid pFiber contains the MAV-1 DNA fragment from nt 2118 to 2384 inserted into pBluescript II SK$^-$ (Stratagene) and is the fiber gene (L5) sequence (6, 40). pZU14 is an E3 cDNA clone that hybridizes to E3, fiber, and pVIII messages. An rRNA-specific oligonucleotide (5) was used as a probe to correct for loading error between samples in the quantitation process. Relative amounts of E3, fiber, and pVIII messages were determined for each virus by quantitating the Northern blots with a Molecular Dynamics model 425E Phosphorimager (Molecular Dynamics, Sunnyvale, Calif.).

Reverse transcription. Ten micrograms of total RNA was treated with 3 U of RNase-free RQ1 DNase (Promega) to remove any contaminating genomic DNA, extracted with phenol, and ethanol precipitated. The RNA was then

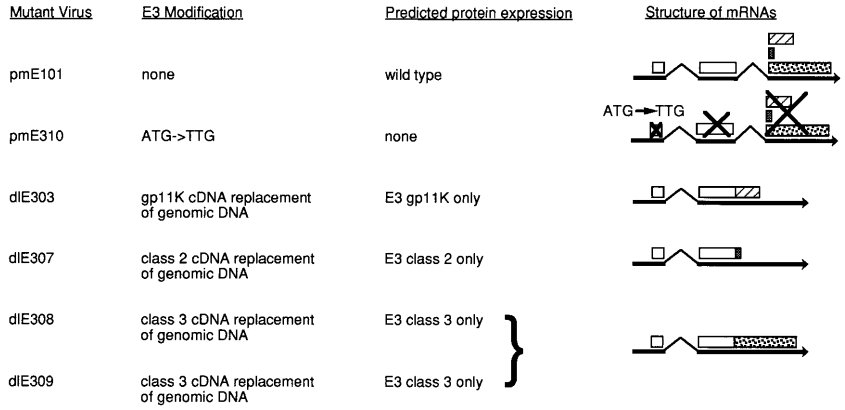

FIG. 2. Predicted message and protein structure of viral recombinants and wt MAV-1. Thick lines, mRNA; angles, introns. Open boxes, amino acid sequences contained in all three E3 proteins; shaded, hatched, and stippled boxes, amino acid sequences unique to each class of E3 protein.

reverse transcribed by using 16 U of avian myeloblastosis virus reverse transcriptase (Promega) in a reaction volume of 50 μl containing 50 mM Tris-HCl (pH 8.3), 50 mM KCl, 10 mM $MgCl_2$, 0.5 mM spermidine, 10 mM dithiothreitol, 0.2 mM deoxynucleoside triphosphates (dNTPs), 80 U RNasin (Promega), and 40 pmol of oligo(dT) (Pharmacia) at 42°C for 90 min. The reverse transcriptase was inactivated by incubation at 94°C for 10 min, and 2 μl of the resulting product was used in each reverse transcriptase (RT) PCR.

PCR. PCR was used to verify the genomic structure of the viral recombinants. Viral DNA was purified by boiling 100 μl of virus stock for 5 min and then mixing with 10 μl of StrataClean resin (Stratagene). The resin was pelleted, and 2 μl of the supernatant was used in each PCR. Primers MAVR1098 (TGTGCCTGCT TCTACTC, oligonucleotide C in Fig. 1) and MAVR1508 (ACGCTGCTGTTA GAAAC, oligonucleotide G in Fig. 1) were used to amplify the E3 region around the second intron to verify the deletions in *dl*E303, *dl*E307, and *dl*E309. Primers MAVRneg27 (GGAAACCTTACAAAGGC, oligonucleotide A in Fig. 1) and MAVR1508 were used to amplify the initiator mutant *pm*E310. This amplified product was then digested with *Hin*dIII to verify the mutation. Primers were annealed at 44°C, and reactions were amplified for 29 cycles. All mutant viruses were also verified by sequencing the region containing the deletions or point mutations by fmol sequencing (Promega). Reverse-transcribed DNA was amplified with a primer specific for each class of E3 message and a primer that annealed upstream of the first intron (MAVR851 [CATCAGCTACAACTAG CAGG, oligonucleotide B in Fig. 1]). This enabled us to distinguish between DNA transcribed from mRNA and contaminating genomic DNA. The E3 class-specific primers were as follows: MAVRC1, GGTACAGGGCAATACTGGCG (gp11K specific); MAVRC2, GGCAATACTGGTTGTACATAC (class 2 specific); and MAVRC3, CAGAAGGTACAGGGCAATACG (class 3 specific) (oligonucleotides D, E, and F, respectively, in Fig. 1). Differential annealing temperatures were 55°C for gp11K-specific amplification, 53°C for class 2-specific amplification, and 63°C for class 3-specific amplification. All reactions were for 29 cycles and carried out in a reaction volume of 25 μl containing 50 mM KCl, 10 mM Tris-HCl (pH 9.0), 0.1% Triton X-100, 0.5 mM $MgCl_2$, 1 U of *Taq* polymerase (Promega), 0.2 mM dNTPs, and 250 ng of each primer.

Electron microscopy. Virus stocks were prepared for transmission electron microscopy by the EM Facility at the University of Georgia College of Veterinary Medicine. Samples were negatively stained with 2% phosphotungstic acid, pH 7.0, and viewed on a JEOL JEM 1201 transmission electron microscope at a beam strength of 80 kV.

Cell labeling and immunoprecipitation. A multiple antigenic peptide (Eall3) containing an amino acid sequence common to all three MAV-1 E3 proteins (FAQKTKWENSR) was synthesized by the University of Georgia Molecular Genetics Instrumentation Facility. This peptide was used to immunize rabbits (University of Georgia Animal Resource Facility) to obtain an antiserum (α-Eall3) that was specific for all three E3 proteins. Cell labeling and immunoprecipitation were performed as described previously (7) and used α-Eall3 antiserum to precipitate E3 proteins and α-EIA (38) to detect MAV-1 E1A. Proteins were visualized on a Molecular Dynamics model 425E Phosphorimager (Molecular Dynamics, Sunnyvale, Calif.). Endoglycosidase H digestions were as previously described (7).

Mouse infections. Virus stocks were diluted in conditioned tissue culture media and injected intraperitoneally into adult NIH Swiss outbred mice (NIHS) obtained from Harlan Sprague Dawley, Inc. The mice were monitored for clinical signs and death for 21 days. Surviving mice were euthanized at 8 weeks postinfection, and the sera were tested for antibodies to MAV-1 by enzyme-linked immunosorbent assay (ELISA) (Charles River) using the manufacturer's protocol.

RESULTS

Mutagenesis of the E3 region of MAV-1. The E3 region of MAV-1 encodes three mRNAs capable of producing three different proteins. The genomic structure of E3 and surrounding regions of MAV-1 prevented straightforward deletion mutagenesis of E3. The predicted mRNA for late protein pVIII is transcribed through the E3 region, and the C-terminal amino acid sequence of this protein is in the same frame as the N-terminal amino acid sequence of E3 (6, 40). Because of this overlap any disruption of the N-terminal half of E3 would also affect pVIII. A possible splice site acceptor and initiation codon for the late protein fiber are immediately downstream of the E3 polyadenylation signal (6, 40). The close proximity of these fiber sequences restricted the possible deletion of the C terminus of the E3 region. cDNA fragments were used to replace genomic sequence to make specific deletions of the second intron such that only a single class of E3 message could be produced. This enabled us to disrupt normal E3 protein production while not disrupting the flanking late protein transcription units.

An *Eco*NI-*Bst*BI DNA fragment was isolated from a cDNA clone encoding E3 gp11K mRNA (Fig. 1). This fragment contained the sequence corresponding to the spliced junction of the second and third exons, resulting in the C-terminal amino acid sequence that is unique to gp11K. This fragment was inserted into an *Eco*NI-*Bst*BI-digested plasmid containing the MAV-1 genomic sequence of the E3 region. The resulting E3 sequence was identical to wt sequence except that the second intron specific for gp11K mRNA had been deleted. This deletion removed the potential for differential splicing and therefore eliminated the possibility that messages encoding class 2 or class 3 could be produced. Similar plasmid constructs were made by using fragments from class 2 and class 3 cDNAs. By using oligonucleotide site-directed mutagenesis, a fourth mutant plasmid, in which the two potential initiator methionines (amino acids 1 and 4) were mutated to leucines (ATG→TTG), was constructed. This conservative amino acid change (9) was made to eliminate translational initiation of the E3 transcripts while preserving the amino acid sequence of pVIII.

The E3 mutant plasmids were then recombined into the virus genome. A critical tool for this recombination was a MAV-1 point mutant virus that we constructed, *pm*E101, that contained a unique restriction site in the E3 region. Wild-type MAV-1 contains two *Eco*RI restriction sites, one in the E1B region and one in E3. A plasmid containing the genomic sequence of E1B was altered by site-directed mutagenesis to abolish the *Eco*RI restriction site while preserving the E1B coding sequence. Single-stranded DNA from this plasmid was annealed to a MAV-1 genomic viral DNA-protein complex that had been partially digested with exonuclease III. This DNA was then transfected into mouse L929 cells. Seventy-eight plaques were obtained and screened for the presence of the mutation by Southern blot and restriction digests of the viral DNA. Only one plaque contained virus that lacked the E1B *Eco*RI site. It was plaque-purified three times, confirmed by sequencing, and designated *pm*E101. This virus was identical to wt MAV-1 in all respects assayed to date and was used as wt in all further experiments.

*pm*E101 DNA-protein complex was digested with *Eco*RI and partially filled in by using Klenow and dATP to prevent religation of the cohesive ends. This digested complex was cotransfected with E3 mutant plasmids into mouse 3T6 cells. The resulting recombinant mutant viruses are listed in Fig. 2. The genomic deletions were verified by PCR using primers that flanked the second intron of E3 (Fig. 1 and 3A). The deletion mutants yielded smaller amplification products (Fig. 3A, lanes 1 to 3) compared with wt virus (Fig. 3A, lane 4), as expected. The ATG→TTG mutant was verified by *Hin*dIII digestion of PCR products obtained with primers that flanked the 5′ end of the E3 coding region (Fig. 3B). The amplified product from the initiator mutant *pm*E310 contained the diagnostic *Hin*dIII restriction site introduced by the mutagenesis (Fig. 3B, lane 1). All mutants were confirmed by sequencing and were found to contain the proper deletions or point mutations (data not shown). *dl*E303 and *dl*E307 grew on mouse 3T6 cells to titers that were 10- to 50-fold lower than wt and produced slightly smaller plaques than wt. *dl*E309 and *pm*E310 exhibited growth characteristics that were identical to wt.

RNA expression during mutant virus infections. The mutants were analyzed for mRNA expression by RT-PCR using primers that were specific for each class of E3 message (Fig. 4). RNA was harvested from equal multiplicities of infection of mouse 3T6 cells with each mutant and then reverse transcribed with an oligo(dT) primer. The resulting DNA was then PCR

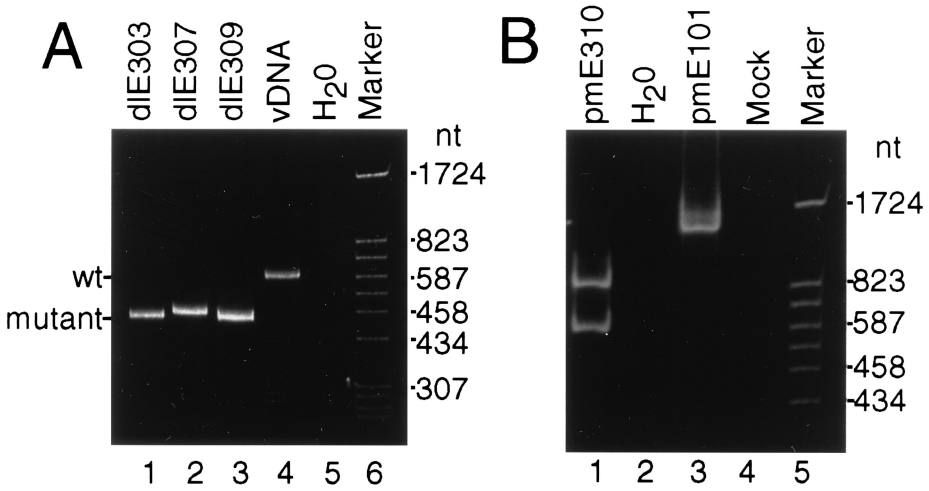

FIG. 3. Genomic PCR of viral mutants. (A) Amplification of the genomic region containing the second intron of MAV-1 E3 from DNA isolated from cells infected with the indicated mutants (primers MAVR1098 and MAVR1508). Smaller bands (lanes 1 to 3) indicate the specific deletions of 158, 148, and 162 bp in *dl*E303, *dl*E307, and *dl*E309 respectively. Wild-type (*pm*E101) genomic DNA from a purified virus amplification product (lane 4) is shown for size comparison. Lane 5, PCR mixture containing no DNA. (B) Amplified products that span the region of translation initiation were digested with *Hin*dIII to test for the ATG→TTG mutation in *pm*E310 (primers MAVRneg27 and MAVR1508). Presence of the 917- and 618-bp digestion products (lane 1) was diagnostic for the incorporation of the point mutations (see the text). Lane 2, PCR mixture containing no DNA; lane 4, PCR mixture containing DNA from mock-infected cells. Sizes of markers are indicated on the right.

amplified with a primer specific for only one class of E3 coding sequence in the region of the second intron deletion and a common primer that hybridizes to a sequence upstream of the first intron (Fig. 1). These primer pairs allowed the differential amplification of sequences that were diagnostic for the expected mRNA expression from each mutant. *dl*E303 produced E3 mRNA capable of encoding only gp11K; *dl*E307 produced E3 mRNA capable of encoding only class 2 protein; *dl*E309 produced E3 mRNA capable of encoding only class 3 protein; *pm*E310 and *pm*E101 produced E3 mRNAs capable of encoding all three E3 proteins as expected (Fig. 4). The lower intensities of class 2 and class 3 signals in *pm*E101 correlates with the lower abundance of clones representing these messages in a cDNA library from MAV-1-infected cells (6). Smaller amplification products were observed in some RT-PCRs of the deletion mutants (Fig. 4, asterisks). These smaller products, which were seen in amplifications from all three mutants in various experiments (data not shown), were isolated and sequenced. The sequences indicated that the products corresponded to splicing resulting from the activation of a cryptic splice acceptor site at nt 1234. In mRNAs in which this acceptor is used, the first intron spans from nt 932 to 1234 instead of from nt 932 to 1085 (6). Larger amplification products (Fig. 4B and C) resulted from the amplification of either unspliced mRNA or genomic DNA contamination and were not reproducible.

We tested the possibility that the decreased titers of *dl*E303 and *dl*E307 were not due to the deletions themselves but rather to negative effects on expression of the late messages that flank the E3 region. Northern blot analysis was used to investigate this possibility (Fig. 5). Total RNAs were isolated from mutant and wt infections and analyzed with probes specific for fiber (Fig. 5A), pVIII (Fig. 5B), or rRNA (data not shown). Signals were quantitated and normalized to the rRNA probe to correct for loading error. Although the deletion mutants produced more fiber and pVIII mRNAs than wt (see Discussion), all of the mutants produced late mRNAs that were the same size and in the same fiber/pVIII ratio as wt late mRNAs (Fig. 5; compare lanes 2, 4, 6, and 8 with lanes 10). These results suggest that the growth defects seen were not due to altered expression of these late messages.

Electron microscopy of mutant virus particles. Additional evidence for proper late structural protein expression was obtained by viewing the virus particles directly by transmission electron microscopy. Representative pictures of each mutant are shown in Fig. 6. All of the mutants have a structure identical to that of wt within the resolution of this technique (Fig. 6; compare *pm*E101 with mutant viruses).

Protein expression in mutant virus infections. The proteins predicted to be produced by each of the mutants are represented in Fig. 2. These predictions were tested by immunoprecipitation of E3 proteins from infected cell lysates. To facilitate this analysis a multiple antigenic peptide that contained 12 amino acids common to all three E3 proteins (amino acids 62 to 73) was synthesized. This peptide was used to produce an antiserum (α-Eall3) in rabbits that could immunoprecipitate each of the three E3 proteins from in vitro transcription/translation reactions (data not shown). Lysates from [^{35}S]Cys-labeled cells that had been mock infected, infected with one of the E3 mutants, or infected with wt virus were precipitated with α-Eall3 immune serum. Precipitated proteins were mock treated or treated with endo H and electrophoresed (Fig. 7). Precipitated protein from cells infected with *dl*E303 (gp11K only) migrated at a molecular size of 14K and was sensitive to endo H (Fig. 7, lanes 1 and 2). These characteristics were consistent with those previously described for gp11K (7). Protein precipitated from cells infected with *dl*E307 (class 2 only) migrated at a molecular weight consistent with the predicted size of a glycosylated class 2 E3 protein (Fig. 7, lane 3). This class 2 protein was sensitive to endo H (Fig. 7, lane 4), indicating that it is N glycosylated and may be retained in the endoplasmic reticulum like gp11K (7). No immunoreactive proteins were detected in lysates from cells infected with *dl*E309 by the α-Eall3 immune serum (Fig. 7, lanes 5 and 6). That these cells were productively infected is supported by the presence of MAV-1 E1A protein in the *dl*E309-infected cell lysate (Fig. 7, lane 13). E3 class 3 proteins were not detected in an independently derived mutant *dl*E308, capable of expressing only class 3 (data not shown). Lysates from cells infected with *pm*E310 (ATG→TTG) contained small amounts of gp11K (Fig. 7, lanes 7 and 8), indicating that there was some

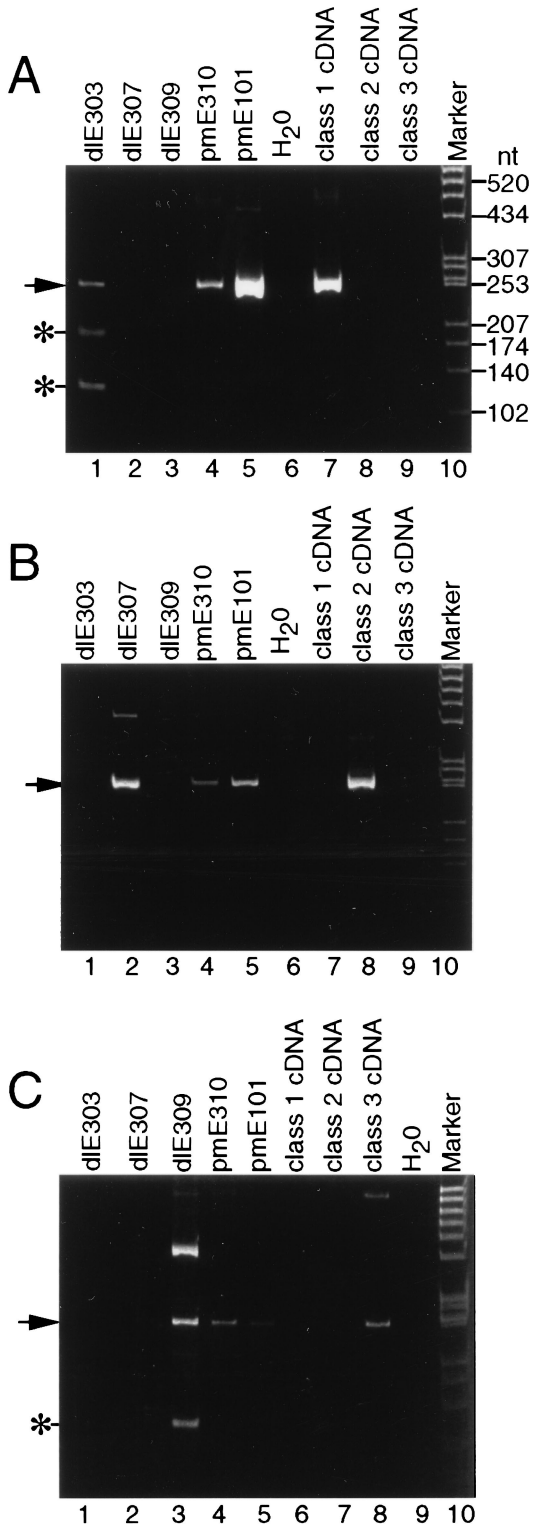

FIG. 4. RT-PCR of viral RNA from infected mouse 3T3 cells. Amplification of reverse-transcribed DNA from cells infected with either *dl*E303, *dl*E307, *dl*E309, *pm*E310, or *pm*E101 (lanes 1 to 5, respectively). cDNA controls for gp11K, class 2, and class 3 were pZ70, pZ50, and pZ333.6 (lanes 7 to 9, respectively). Lane 6, PCR mixture containing no DNA. (A) Amplification using primers specific for gp11K messages (primers MAVRC1 and MAVR851); (B) amplification using primers specific for class 2 messages (primers MAVRC2 and MAVR851); (C) amplification using primers specific for class 3 messages (primers MAVRC3 and MAVR851). Expected amplification products are indicated by arrows. Smaller amplification products (asterisks) are a result of novel splicing (see the text). Sizes of markers are indicated.

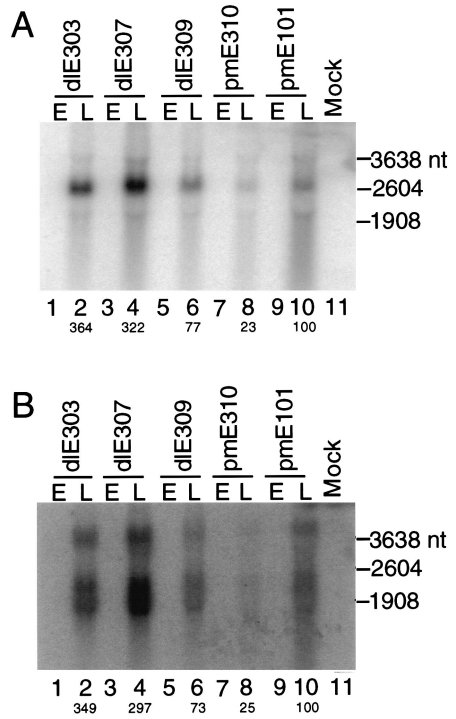

FIG. 5. Northern blot analysis of RNA from infected mouse 3T6 cells. Twenty micrograms of total RNA harvested from cells at 22 (E) or 44 (L) h postinfection with each of the indicated mutants was separated on a 1% agarose gel and blotted to nitrocellulose. The blot was probed with either a fiber-specific probe (A) or a pVIII-specific probe (B). Sizes of RNA markers are shown on the right. Quantities of mRNA relative to wt (100%) are shown below. The ratios of fiber to pVIII were as follows: *dl*E303, 1.04; *dl*E307, 1.09; *dl*E309, 1.06; *pm*E310, 0.92; *pm*E101, 1.00.

translation from the mutated E3 initiator in this virus. Lysates from cells infected with wt (*pm*E101) virus produced only gp11K at detectable levels (Fig. 7, lanes 9 and 10).

Mutant viruses have greater LD_{50}s than wt virus in outbred Swiss mice. The effects of the E3 mutations on the pathogenesis of MAV-1 were measured by determining the 50% lethal dose (LD_{50}) for each mutant in NIH Swiss outbred mice. Serial dilutions of each mutant and wt virus were used to infect 5- to 8-week-old male mice intraperitoneally. The mice showed signs of MAV-1 infection that were consistent with those previously reported (28, 36). The LD_{50}s were calculated (41) and are shown in Table 1. Two separate trials were conducted and produced similar results. The second trial included higher dilutions of *pm*E101 (wt) and a lower dilution of *dl*E309 (class 3 only) to obtain precise LD_{50}s of these viruses. An independently derived class 3 mutant, *dl*E308, was also used in the second trial and produced results that were similar to those obtained with *dl*E309. *pm*E101 (wt) had an LD_{50} of less than 1 PFU, comparable to the LD_{50} for wt MAV-1 (36). This suggests that the cell culture plaque assay used to determine the titers of these viruses may not accurately reflect the actual number of infectious particles for mice present in the stocks. Previous studies have indicated that MAV-1 has a particle/PFU ratio of approximately 1,000 (47). Surviving mice were tested 2 to 8 months after injection for the presence of MAV-1-specific antibodies, and most were found to be seropositive. A low percentage of mice (<5%) that received the lowest doses of mutant virus failed to seroconvert (data not shown).

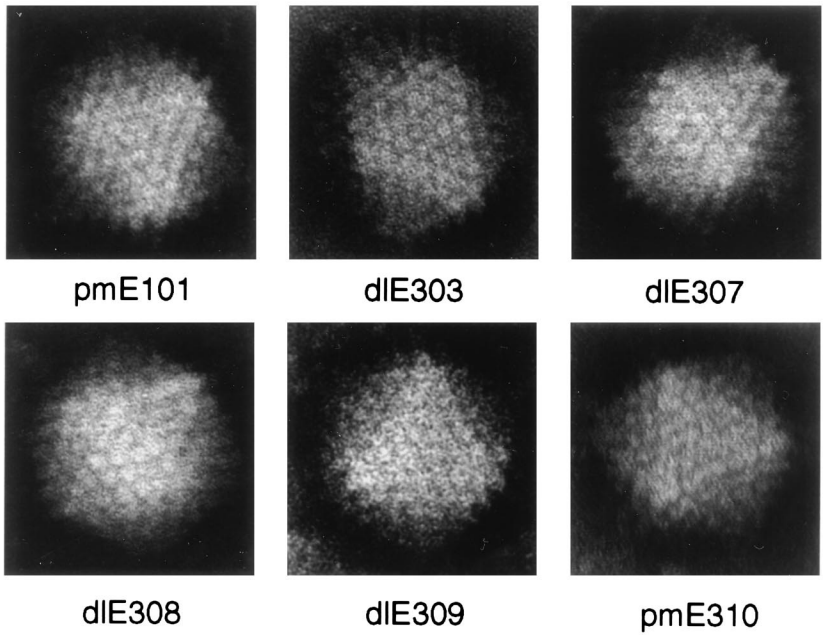

FIG. 6. Transmission electron microscopy of viral mutants and wt MAV-1. Virus stocks from infected mouse 3T6 cells were negatively stained. Magnification, ×335,000.

DISCUSSION

We have used directed mutagenesis of MAV-1 to construct viral recombinants that contain mutations of the E3 region. These mutations resulted in the expression of reduced levels of protein from the E3 region or expression of only one of the three possible E3 proteins. The altered protein production of these recombinant viruses resulted in a decreased pathogenicity in outbred Swiss mice.

All of the E3 mutants constructed grew in cell culture, indicating that the E3 proteins are not essential for viral replication in culture. Two mutants, *dl*E303 and *dl*E307, grew to titers that were 10- to 50-fold lower than that of wt virus. Several observations have indicated that the lower titers of these viruses may be due to an impaired ability of these viruses to form plaques. Northern blots (Fig. 4) were performed with RNA from cells that were infected with equal multiplicities of infection based on plaque titers. The increased levels of all viral RNAs examined for the *dl*E303 and *dl*E307 mutants (Fig. 3 and data not shown) suggest that these virus stocks contained a larger number of infectious particles than indicated by the plaque assay. Further evidence for this was obtained during the electron microscopy study of the various virus stocks. All of the preparations of the virus stocks contained similar numbers of particles when viewed by electron microscopy or quantitated by DNA content, although the *dl*E303 and *dl*E307 titers as determined by plaque assays were 10- to 50-fold lower than wt (data not shown). Further studies are in progress to investigate the plaquing efficiency, small plaque phenotype, and particle/PFU ratios of these mutants.

Mutant *pm*E310 contains two point mutations that change the potential initiator methionine codons (ATG) to leucine codons (TTG). Surprisingly, this mutant was able to produce small amounts of E3 proteins. Nonmitochondrial translational

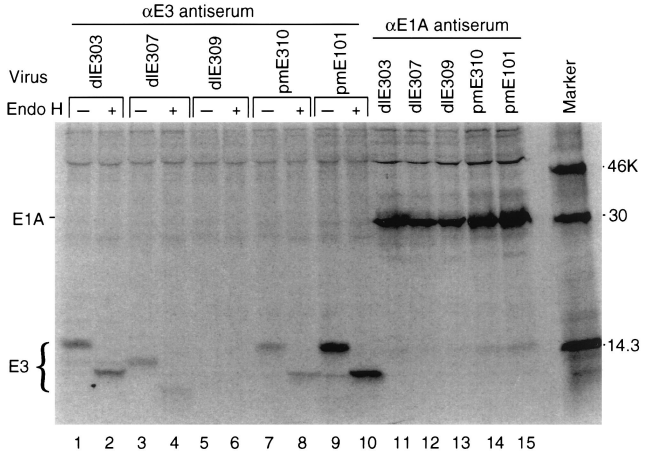

FIG. 7. Immunoprecipitation of ^{35}S-labeled E3 proteins from mutant- or wt-infected mouse 3T6 cells. Proteins were precipitated with α-Eall3 antisera and either mock treated (−) or treated (+) with endoglycosidase (+) (lanes 1 to 10). Proteins were precipitated with α-E1A antisera as a control for virus infection (lanes 11 to 15). Proteins were electrophoresed on a 10 to 18% gradient sodium dodecyl sulfate-polyacrylamide gel and visualized on a Phosphorimager. Sizes of protein markers are indicated on the right.

TABLE 1. E3 mutant virus LD_{50}s

Virus	LD_{50} (log PFU)[a]	
	Trial 1	Trial 2
*pm*E101	<0	−0.8
*pm*E310	1.8	1.2
*dl*E303	3.8	3.5
*dl*E307	3.4	3.8
*dl*E309	>4	4.7
*dl*E308	ND[b]	4.0

[a] Determined from two independent infections of adult NIHS Swiss outbred mice. Six mice per dose were inoculated intraperitoneally with the indicated viruses at 10-fold serial dilutions. Mice were monitored for 21 days postinfection for mortality. LD_{50}s were calculated by the method of Reed and Muench (41).

[b] ND, not determined.

initiation in eukaryotes from TTG codons has been reported (29, 54), and we believe that this type of initiation event is responsible for the low levels of translation in *pm*E310. *dl*E303 and *dl*E307 expressed the expected single E3 proteins of the appropriate size. However, *dl*E308 and *dl*E309 did not produce any E3 proteins detectable by immunoprecipitation. Cells infected with *pm*E101 produced only gp11K at detectable levels. This expression pattern is consistent with the fact that gp11K mRNAs appear to be present at higher levels in infected cells compared with class 2 and class 3 mRNAs. This greater abundance of gp11K mRNA has been suggested by the higher relative number of gp11K clones in a cDNA library from infected cells (6) and the stronger gp11K signal in RT-PCR of RNA from wt-infected cells (Fig. 4, lanes 5). The relative abundance of all spliced mRNAs and thus the relative protein levels of MAV-1 E3 may be dependent on the tissue or cell type. Cell-specific splicing control has been seen in transgenic mice expressing the human adenovirus E3 (20). It is possible that, during MAV-1 infections of mice, each class of E3 protein is more abundantly expressed in a certain tissue type where it plays a specific role.

All of the mutations of MAV-1 E3 resulted in a decreased pathogenicity in outbred Swiss mice. This observation suggests that these proteins have an important role in the life cycle of the virus in its natural host. *pm*E310 had an LD_{50} that was only slightly greater than the LD_{50} of wt virus. *pm*E310 is capable of producing gp11K and presumably also the other two E3 proteins at low levels. The lower LD_{50} of this virus implies that the quantities of the E3 proteins are an important determinant of the pathogenesis of the virus. Two mutants, *dl*E303 and *dl*E307, had similar increases in LD_{50}s relative to wt. Because both of these mutants lack the ability to express the class 3 protein, it is possible that this decreased lethality is due to the lack of the class 3 protein. *dl*E308 and *dl*E309 are independently derived mutants capable of expressing only class 3 proteins. These viruses had the most impaired ability to cause disease in the mice, as indicated by the greatest LD_{50}s. It is difficult to predict the importance of each E3 protein in the pathogenesis of the virus on the basis of the LD_{50} experiments presented here. However, these experiments suggest that more than one of the three E3 proteins is essential for normal disease production in the natural host.

The E3 mutant viruses were tested in vivo by intraperitoneal injection, the commonly used route of experimental MAV-1 inoculation. Little is known about the natural route of transmission of MAV-1. Evidence suggests that natural transmission requires direct contact with infected animals. Thirty-five percent of uninoculated mice housed in the same cage with artificially infected mice developed antibodies to MAV-1, while no mice housed in separate cages in the same room seroconverted (30). After intraperitoneal inoculation, the virus spreads throughout the mouse and can be isolated from the kidney, heart, spleen, brain, adrenal glands, pancreas, and liver (8, 31). In adult outbred Swiss NIHS mice the highest levels of MAV-1 viral DNA are detected in the spleen and brain (36). MAV-1 infection results in an acute central nervous system disease producing ataxia, tremor, and paralysis in infected mice (28, 36). Histological analysis of tissue samples from mice showing signs of MAV-1 central nervous system disease were consistent with these clinical signs. MAV-1 infection of adult, immunocompetent mice can also result in a persistent infection characterized by high serum antibody titers and prolonged viruria (42, 51). It will be interesting to determine whether the E3 mutant viruses exhibit altered tissue tropism or an altered ability to establish or maintain a persistent infection.

Disruption of normal MAV-1 E3 protein expression has a dramatic effect on the pathogenicity of the virus. This finding fits well with the observation that the variation between different adenovirus E3 regions correlates with the different types of pathogenesis in these viruses. The correlation of loss of E3 functions to a decrease in the virulence of MAV-1 in its natural host is similar to what is seen in the canine adenovirus, CAV-1, the causative agent of infectious canine hepatitis. The attenuated vaccine strain of CAV-1 and the wt CAV-1 replicate equally well in cultured cells, yet the vaccine strain is nonpathogenic in the animal. The only known difference between these two strains is that the vaccine strain has a large deletion in the E3 region (17, 18). The effects of E3 deletions on pathogenicity in both MAV-1 and CAV-1 are contrary to the results obtained by using human adenovirus mutants to infect animal models, in which the deletion of E3 results in increased virulence. This difference could indicate that the E3 proteins of different adenoviruses have evolved to perform very specific functions that are unique in the pathogenicity of each virus in its host. Alternatively, discrepancies between the results for MAV-1 and CAV-1 compared with human adenovirus in mice may be due to the fact that the latter is a heterologous, nonreplicative model.

Further studies using these mutant viruses and wt MAV-1 to infect mice that have specific immune system deficiencies will enable a complete analysis of the MAV-1 E3 proteins and their functions. The ability to construct viral recombinants that can be used to infect the natural host, combined with the vast potential of the mouse as a research animal, should provide valuable insight into how the E3 proteins contribute to the pathogenicity of adenoviruses.

ACKNOWLEDGMENTS

We are grateful to Charles W. Beard, Angela N. Cauthen, Gwen Hirsch, Susan C. Kring, Liz LaRue, Julie A. Olszewski, Kimberley Smith, and Baoling Ying for helpful discussions, technical assistance, and critical reviews. We thank Chris King of the UGA Animal Resources Facility for help with the mouse trials and Lois Miller, Rich Meagher, and Sidney Kushner for comments on the manuscript.

This work was supported by NIH grant RO1 AI 23762 to K.R.S. and in part by NIH predoctoral traineeship GM07103 to C.W.B. K.R.S. is the recipient of an NIH Research Career Development Award.

REFERENCES

1. **Andersson, M., S. Pääbo, T. Nilsson, and P. A. Peterson.** 1985. Impaired intracellular transport of class I MHC antigens as a possible means for adenoviruses to evade immune surveillance. Cell **43:**215–222.
2. **Bailey, A., and V. Mautner.** 1994. Phylogenetic relationships among adenovirus serotypes. Virology **205:**438–452.
3. **Ball, A. O., C. W. Beard, S. D. Redick, and K. R. Spindler.** 1989. Genome organization of mouse adenovirus type 1 early region 1: a novel transcription map. Virology **170:**523–536.
4. **Ball, A. O., M. E. Williams, and K. R. Spindler.** 1988. Identification of mouse adenovirus type 1 early region 1: DNA sequence and a conserved transactivating function. J. Virol. **62:**3947–3957.
5. **Barbu, V., and F. Dautry.** 1989. Northern blot normalization with a 28S rRNA oligonucleotide probe. Nucleic Acids Res. **17:**7115.
6. **Beard, C. W., A. O. Ball, E. H. Wooley, and K. R. Spindler.** 1990. Transcription mapping of mouse adenovirus type 1 early region 3. Virology **175:**81–90.
7. **Beard, C. W., and K. R. Spindler.** 1995. Characterization of an 11K protein produced by early region 3 of mouse adenovirus type 1. Virology **208:**457–466.
8. **Blailock, Z. R., E. R. Rabin, and J. L. Melnick.** 1967. Adenovirus endocarditis in mice. Science **157:**69–70.
9. **Bordo, D., and P. Argos.** 1991. Suggestions for "safe" residue substitutions in site-directed mutagenesis. J. Mol. Biol. **217:**721–729.
10. **Burgert, H.-G., and S. Kvist.** 1985. An adenovirus type 2 glycoprotein blocks cell surface expression of human histocompatibility class I antigens. Cell **41:**987–997.
11. **Burgert, H.-G., and S. Kvist.** 1987. The E3/19K protein of adenovirus type 2 binds to the domains of histocompatibility antigens required for CTL recognition. EMBO J. **6:**2019–2026.
12. **Burgert, H.-G., J. L. Maryanski, and S. Kvist.** 1987. "E3/19K" protein of

adenovirus type 2 inhibits lysis of cytolytic T lymphocytes by blocking cell surface expression of histocompatibility class I antigens. Proc. Natl. Acad. Sci. USA **84:**1356–1360.
13. **Cai, F., D. Tang, and J. M. Weber.** 1992. Primary structure of the murine adenovirus type 1 proteinase. Biochim. Biophys. Acta **1129:**339–341.
14. **Carlin, C. R., A. E. Tollefson, H. A. Brady, B. L. Hoffman, and W. S. M. Wold.** 1989. Epidermal growth factor receptor is down-regulated by a 10,400 MW protein encoded by the E3 region of adenovirus. Cell **57:**135–144.
15. **Cauthen, A. N., and K. R. Spindler.** 1996. Sequence of the mouse adenovirus type-1 DNA encoding the 100-kDa, 33-kDa and DNA binding proteins. Gene **168:**183–187.
16. **Cox, J. H., M. L. Buller, J. R. Bennink, J. W. Yewdell, and G. Karupiah.** 1994. Expression of adenovirus E3/19K protein does not alter mouse MHC class I-restricted responses to vaccinia virus. Virology **204:**558–562.
17. **Dragulev, B., S. Sira, M. G. AbouHaidar, and J. B. Campbell.** 1990. Analysis of the E3 region of canine adenovirus type 1: comparison of an unattenuated and a vaccine strain, p. 145. *In* VIIIth International Congress of Virology abstracts.
18. **Dragulev, B. P., S. Sira, M. G. AbouHaidar, and J. B. Campbell.** 1991. Sequence analysis of putative E3 and fiber genomic regions of two strains of canine adenovirus type 1. Virology **183:**298–305.
19. **Dunsworth-Browne, M., R. E. Schell, and A. J. Berk.** 1980. Adenovirus terminal protein protects single stranded DNA from digestion by a cellular exonuclease. Nucleic Acids Res. **8:**543–554.
20. **Fejer, G., I. Gyory, J. Tufariello, and M. S. Horwitz.** 1994. Characterization of transgenic mice containing adenovirus early region 3 genomic DNA. J. Virol. **68:**5871–5881.
21. **Flomenberg, P., J. Szmulewicz, E. Gutierrez, and H. Lupatkin.** 1992. Role of the adenovirus E3-19k conserved region in binding major histocompatibility complex class I molecules. J. Virol. **66:**4778–4783.
22. **Ginsberg, H. S., U. Lundholm-Beauchamp, R. L. Horswood, B. Pernis, W. S. M. Wold, R. M. Chanock, and G. A. Prince.** 1989. Role of early region 3 (E3) in pathogenesis of adenovirus disease. Proc. Natl. Acad. Sci. USA **86:**3823–3827.
23. **Ginsberg, H. S., L. L. Moldawer, P. B. Sehgal, M. Redington, P. L. Kilian, R. M. Chanock, and G. A. Prince.** 1991. A mouse model for investigating the molecular pathogenesis of adenovirus pneumonia. Proc. Natl. Acad. Sci. USA **88:**1651–1655.
24. **Gooding, L. R., L. W. Elmore, A. E. Tollefson, H. A. Brady, and W. S. M. Wold.** 1988. A 14,700 MW protein from the E3 region of adenovirus inhibits cytolysis by tumor necrosis factor. Cell **53:**341–346.
25. **Gooding, L. R., T. S. Ranheim, A. E. Tollefson, L. Aquino, P. Duerksen-Hughes, T. M. Horton, and W. S. M. Wold.** 1991. The 10,400- and 14,500-dalton proteins encoded by region E3 of adenovirus function together to protect many but not all mouse cell lines against lysis by tumor necrosis factor. J. Virol. **65:**4114–4123.
26. **Gorman, C., R. Padmanabhan, and B. H. Howard.** 1983. High efficiency DNA-mediated transformation of primate cells. Science **221:**551–553.
27. **Grunhaus, A., S. Cho, and M. S. Horwitz.** 1994. Association of vaccinia virus-expressed adenovirus E3-19K glycoprotein with class I MHC and its effects on virulence in a murine pneumonia model. Virology **200:**535–546.
28. **Guida, J. D., G. Fejer, L.-A. Pirofski, C. F. Brosnan, and M. S. Horwitz.** 1995. Mouse adenovirus type 1 causes a fatal hemorrhagic encephalomyelitis in adult C57BL/6 but not BALB/c mice. J. Virol. **69:**7674–7681.
29. **Guss, B., M. Eliasson, A. Olsson, M. Uhlén, A. K. Frej, H. Jornvall, J.-I. Flock, and M. Lindberg.** 1986. Structure of the IgG-binding regions of streptococcal protein G. EMBO J. **5:**1567–1575.
30. **Hartley, J. W., and W. P. Rowe.** 1960. A new mouse virus apparently related to the adenovirus group. Virology **11:**645–647.
31. **Heck, F. C., Jr., W. G. Sheldon, and C. A. Gleiser.** 1972. Pathogenesis of experimentally produced mouse adenovirus infection in mice. Am. J. Vet. Res. **33:**841–846.
32. **Hirt, B.** 1967. Selective extraction of polyoma DNA from infected mouse cell cultures. J. Mol. Biol. **26:**365–369.
33. **Kelly, T. J., Jr., and A. M. Lewis, Jr.** 1973. Use of nondefective adenovirus-simian virus 40 hybrids for mapping the simian virus 40 genome. J. Virol. **12:**643–652.
34. **Kerr, C., and P. D. Sadowski.** 1972. Gene 6 exonuclease of bacteriophage T7. J. Biol. Chem. **247:**305–318.
35. **Kring, S. C., A. O. Ball, and K. R. Spindler.** 1992. Transcription mapping of mouse adenovirus type 1 early region 4. Virology **190:**248–255.
36. **Kring, S. C., C. S. King, and K. R. Spindler.** 1995. Susceptibility and signs associated with mouse adenovirus type 1 infection of adult outbred Swiss mice. J. Virol. **69:**8084–8088.
37. **Kring, S. C., and K. R. Spindler.** 1990. Sequence of mouse adenovirus type 1 DNA encoding the amino terminus of protein IVa2. Nucleic Acids Res. **18:**4003.
38. **Levine, A. J.** 1984. The adenovirus early proteins. Curr. Top. Microbiol. Immunol. **110:**143–167.
39. **Persson, H., C. Signäs, and L. Philipsson.** 1979. Purification and characterization of an early glycoprotein from adenovirus type 2-infected cells. J. Virol. **29:**938–948.
40. **Raviprakash, K. S., A. Grunhaus, M. A. El Kholy, and M. S. Horwitz.** 1989. The mouse adenovirus type 1 contains an unusual E3 region. J. Virol. **63:**5455–5458.
41. **Reed, L. J., and H. Muench.** 1938. A simple method of estimating fifty per cent endpoints. Am. J. Hyg. **27:**493–497.
42. **Richter, C. B.** 1986. Mouse adenovirus, K virus, pneumonia virus of mice, p. 137–161. *In* P. N. Bhatt, R. O. Jacoby, H. C. I. Morse, and A. E. New (ed.), Viral and mycoplasmic infections of laboratory rodents: effects on biomedical research. Academic Press, New York.
43. **Smith, K., B. Ying, A. O. Ball, C. W. Beard, and K. R. Spindler.** Interaction of mouse adenovirus type 1 early region 1A protein with cellular proteins pRb and p107. Submitted for publication.
44. **Song, B., K. R. Spindler, and C. S. H. Young.** 1995. Sequence of the mouse adenovirus serotype-1 DNA encoding the precursor to capsid protein VI. Gene **152:**279–280.
45. **Southern, E. M.** 1975. Detection of specific sequences among DNA fragments separated by gel electrophoresis. J. Mol. Biol. **98:**503–517.
46. **Sparer, T. E., R. A. Tripp, D. L. Dillehay, T. W. Hermiston, W. S. Wold, and L. R. Gooding.** 1996. The role of human adenovirus early region 3 proteins (gp19K, 10.4K, 14.5K, and 14.7K) in a murine pneumonia model. J. Virol. **70:**2431–2439.
47. **Spindler, K. R.** Unpublished data.
48. **Tollefson, A. E., A. Scaria, T. W. Hermiston, J. S. Ryerse, L. J. Wold, and W. S. M. Wold.** 1996. The adenovirus death protein (E3-11.6K) is required at very late stages of infection for efficient cell lysis and release of adenovirus from infected cells. J. Virol. **70:**2296–2306.
49. **Tufariello, J., S. Cho, and M. S. Horwitz.** 1994. The adenovirus E3 14.7-kilodalton protein which inhibits cytolysis by tumor necrosis factor increases the virulence of vaccinia virus in a murine pneumonia model. J. Virol. **68:**453–462.
50. **Tufariello, J. M., S. Cho, and M. S. Horwitz.** 1994. Adenovirus E3 14.7-kilodalton protein, an antagonist of tumor necrosis factor cytolysis, increases the virulence of vaccinia virus in severe combined immunodeficient mice. Proc. Natl. Acad. Sci. USA **91:**10987–10991.
51. **van der Veen, J., and A. Mes.** 1973. Experimental infection with mouse adenovirus in adult mice. Arch. Gesamte Virusforsch. **42:**235–241.
52. **Weber, J. M., F. Cai, R. Murali, and R. M. Burnett.** 1994. Sequence and structural analysis of murine adenovirus type 1 hexon. J. Gen. Virol. **75:**141–147.
53. **Wold, W. S. M., and L. R. Gooding.** 1991. Region E3 of adenovirus: a cassette of genes involved in host immunosurveillance and virus-cell interactions. Virology **184:**1–8.
54. **Zemmour, J., A.-M. Little, D. J. Schendel, and P. Parham.** 1992. The HLA-A,B "negative" mutant cell line C1R expresses a novel HLA-B35 allele, which also has a point mutation in the translation initiation codon. J. Immunol. **148:**1941–1948.